

hep-ph/0307096

October 9, 2019

SINGLE PHOTON SIGNALS FOR WARPED QUANTUM GRAVITY AT A LINEAR e^+e^- COLLIDER

Santosh Kumar Rai and Sreerup Raychaudhuri

Department of Physics, Indian Institute of Technology, Kanpur 208 01, India

E-mail: skrai@iitk.ac.in, sreerup@iitk.ac.in

ABSTRACT

We study the ‘single photon’ process $e^+e^- \rightarrow \gamma\nu\bar{\nu}$ with contributions due to exchange of massive gravitons in the Randall-Sundrum model of low-scale quantum gravity. It is shown that for significant regions in the parameter space, this process unambiguously highlights the resonance structure of the graviton sector. Even in the non-resonant part of the parameter space, we show that comparison with the benchmark process $e^+e^- \rightarrow \mu^+\mu^-$ can clearly distinguish signals for warped gravity from similar signals for large extra dimensions.

1 Introduction

One of the most exciting theoretical developments of recent years has been the idea that there could be one or more extra spatial dimensions and that the observable Universe could be confined to a four-dimensional hyper-surface in a higher dimensional bulk spacetime [1]. Such ideas, which fit in naturally with current ideas in superstring theory, give rise to elegant solutions to the well-known gauge hierarchy problem of high energy physics. What is even more interesting, perhaps, is the suggestion that there could be observable signals of quantum gravity at current and future accelerator experiments.

This relatively new body of ideas, commonly dubbed ‘Brane World Phenomenology’, bases itself on two main ideas: the concept of hidden compact dimensions [2] and the string-theoretic idea of D -branes [3]. There are two main scenarios, each having variants. One is the so-called Arkani-Hamed-Dimopoulos-Dvali (ADD) model [4], in which there are d more extra spatial dimensions, compactified on a d -torus of radius R_c each way, which, together with the four canonical Minkowski dimensions, constitutes the ‘bulk’ spacetime. In this scenario R_c can be [5] as large as $200 \mu\text{m}$. However, the Standard Model (SM) fields are confined to a four-dimensional slice of spacetime, with thickness not more than $10^{-12} \mu\text{m}$, which is dubbed the ‘brane’. If the model is embedded in a string-theoretic framework, the ‘brane’ is, in fact a D_3 -brane, i.e. a 3+1 dimensional hyper-surface on which the ends of open strings are confined¹. However, gravity, which is a property of spacetime itself, must be free to propagate in the bulk. As a result

- Planck’s constant in the bulk \hat{M}_P is related to Planck’s constant on the brane $M_P (\simeq 1.2 \times 10^{19} \text{ GeV})$ by $\hat{M}_P^{2+d} R_c^d = (4\pi)^{d/2} \Gamma(d/2) M_P^2$ which means that for $R_c \sim 200 \mu\text{m}$, it is possible to have \hat{M}_P as low as a TeV. This solves the gauge hierarchy problem simply by bringing down the scale of new physics (i.e. gravity) to about a TeV.
- There are a huge number of massive Kaluza-Klein excitations of the (bulk) graviton field, as perceived on the brane. These collectively produce effects of electroweak strength, which may be observable at current experiments and those planned in the near future [6, 7, 8].

A major drawback of the ADD model is that it creates a new hierarchy between the ‘string scale’ $\hat{M}_P \sim 1 \text{ TeV}$ and the size of the extra dimensions $R_c^{-1} \sim 1 \mu\text{eV}$. Moreover, it can be argued that the huge (compared with the Planck length) size of the extra dimensions is unstable under quantum corrections, which tend to shrink it down until $\hat{M}_P \sim R_c^{-1} \sim M_P$. This problem is brilliantly solved in the Randall-Sundrum (RS) model [9], which has grown out of the ADD model.

In the RS model, there are *two* branes — a ‘visible’ brane containing the SM fields and an ‘invisible’ brane where gravity is strong (as strong as the electroweak interaction)

¹It is not absolutely essential to embed the model in a string theory, and the word ‘brane’ or ‘wall’ is then used simply to denote a hyper-surface or domain wall where SM fields are confined.

— embedded in a five-dimensional bulk, where the single extra dimension is a $\mathbf{S}^1/\mathbf{Z}_2$ orbifold. i.e. a circle folded about a diameter. Placing the two branes at the two orbifold fixed points $\phi = 0, \pi$, and assuming they have equal and opposite energy densities (brane tensions), which are related to a negative cosmological constant in the bulk, one obtains a ‘warped’ solution to the five-dimensional Einstein equations of the form

$$ds^2 = e^{-\mathcal{K}R_c\phi} g_{\mu\nu} dx^\mu dx^\nu + R_c^2 d\phi^2 \quad (1)$$

where \mathcal{K} is the curvature of the fifth dimension. Gravity is strong on the invisible brane at $\phi = 0$ and weak on the visible brane $\phi = \pi$. It is now possible to choose all the fundamental energy scales in the problem in the ballpark of the Planck scale provided $\mathcal{K}R_c \simeq 12$. This moderate value reduces the ‘warp factor’ $e^{-\mathcal{K}R_c\pi}$ to about 10^{-16} — adequate to explain the hierarchy between electroweak and Planck scales. One thus obtains a natural solution to the hierarchy problem in this model: exponential generation of large/small numbers explains the weakness of the observed gravitational interactions. Of course, this is achieved at the cost of (a) tuning brane tensions with the bulk cosmological constant and (b) assuming negative brane-tension. It is fair to say that the RS model successfully fuses the gauge hierarchy problem with the cosmological constant problem, and presumably both have a common solution.

Phenomenologically, the RS model is rather similar to the ADD model, but there are two important differences. These are

- Each Kaluza-Klein excitation of the bulk graviton has a mass [10, 11]

$$M_n = x_n \mathcal{K} e^{-\mathcal{K}R_c\pi} \equiv x_n m_0 \quad (2)$$

where $m_0 = \mathcal{K} e^{-\mathcal{K}R_c\pi} \sim 100$ GeV is the graviton mass scale and x_n are the zeros of the Bessel function $J_1(x)$ of order unity ($n \in \mathbf{Z}$). This means that the Kaluza-Klein gravitons have masses of a few hundred GeV, unlike the ADD case, where the masses start from ~ 1 μ eV.

- Each Kaluza-Klein excitation of the bulk graviton couples to matter as [11]

$$\kappa e^{\mathcal{K}R_c\pi} = \frac{4\sqrt{\pi}}{M_P} e^{\mathcal{K}R_c\pi} \equiv \frac{4\sqrt{\pi}c_0}{m_0} \quad (3)$$

where $\kappa = \sqrt{16\pi G_N}$ and $c_0 = \mathcal{K}/M_P \simeq 0.01 - 0.1$ is an effective coupling constant, whose magnitude is fixed by (a) naturalness and (b) requiring the curvature of the fifth dimension to be small enough to consider linearized gravity on the ‘visible’ brane.

RS gravitons, thus, resemble weakly-interacting massive particles (WIMPs) in most models, except for (a) the fact that there always exists a tower of graviton Kaluza-Klein modes and (b) these are spin-2 particles. In phenomenological studies of the RS model,

the mass scale m_0 and the ratio c_0 may be treated as free parameters²: they are convenient replacements for the fundamental quantities \mathcal{K} and R_c :

$$\mathcal{K} = c_0 M_P, \quad R_c = \frac{1}{\pi \mathcal{K}} \log \frac{\mathcal{K}}{m_0} \quad (4)$$

Accelerator searches for RS gravitons mainly depend on the resonant structure of graviton-mediated cross-sections. The non-observation of any such effects at LEP-2, for example, constrains $M_1 > 206$ GeV, or $m_0 > 54$ GeV. At a hadron collider, such as the Tevatron or the LHC, one looks [11] for s -channel graviton exchange contributions to simple processes like $p + p(\bar{p}) \rightarrow \ell^+ \ell^-$ or $p + p(\bar{p}) \rightarrow \gamma \gamma$ or the more complicated $p + p(\bar{p}) \rightarrow$ dijets, where one should expect to see graviton resonances in the invariant mass distribution of the final state. The observation of such resonances would certainly be a signal for the RS model. However, it may not be possible to clinch the issue of whether such signals are uniquely due to RS gravitons or to some other form of new physics. The reason is simple: *any* particle exchanged in the s -channel for the above processes, such as, for example, a Z' -boson, would induce very similar signals. In order to verify that an observed resonance is indeed a graviton resonance, we need to (a) measure the position, width and height of the resonance peak, and (b) compare the angular distribution of the final states with that predicted for a spin-2 exchange in the s -channel. While these may, indeed, be possible[11], it must be pointed out that the presence of large irreducible backgrounds at a hadron collider is a serious problem, as it induces large errors in the width and height measurements. It seems natural, then, to turn to a high-energy e^+e^- collider, where the environment is clean and see if one can obtain an unambiguous signal for RS gravity.

Several studies of RS gravitons at e^+e^- colliders may already be found in the literature [12, 13, 14]. For example, one can have s -channel graviton exchanges in $e^+e^- \rightarrow \mu^+ \mu^-, e^+e^-$ and $\gamma \gamma$. In these studies [15] it is shown that if the center-of-mass energy is run over a typical range, say 350 GeV to 1.5 TeV, one gets beautiful resonances at the masses of the RS gravitons, for a suitable choice of parameters. Conversely, if one fixes the energy and runs over the graviton mass parameter m_0 , one again generates resonances whenever the condition $\sqrt{s} \simeq M_n$ is satisfied. However, one must remember that if the RS model is true, then Nature has only one value of m_0 . Moreover, it is likely that the next generation e^+e^- machine will be run (like the LEP) only at certain fixed values of beam energy [16]. It is quite possible, therefore, that the actual machine energy will be an *off-resonance point* for the RS model, in which case, all these cross-sections will show modest enhancements, but no resonant behavior. It may not, then, be easy to distinguish graviton contributions from those due to other forms of ‘new physics’, such as supersymmetry or extra gauge bosons [17].

In this article, we examine the $2 \rightarrow 3$ -body process $e^+e^- \rightarrow \gamma \nu \bar{\nu}$, which is observable as a final state with a single hard transverse photon with unbalanced (missing) energy.

²The alternative choice of $\Lambda_\pi = \overline{M}_P e^{-\mathcal{K} R_c \pi} = m_0 / \sqrt{8\pi c_0}$ instead of m_0 and of $\mathcal{K} / \overline{M}_P = \sqrt{8\pi c_0}$ instead of c_0 may also be found in the literature [11].

Such states are very distinctive and are, in fact, predicted in a wide variety of models beyond the SM [18, 19, 20]. It is likely that some part of the experimental effort at a high-energy e^+e^- collider will be devoted to an analysis of this signal, which is simple, clean and physically interesting. The process can be thought of as a neutrino pair-production with an initial-state radiation (ISR) of a photon. Since this photon carries away a variable amount of energy, it is possible for the remaining system to strike a s -channel graviton resonance, just as ISR at LEP-2 has been seen to cause a ‘radiative return’ to the Z -boson pole. The resonant gravitons can be thought of as real particles, in which case, the basic process is the $2 \rightarrow 2$ -body process $e^+e^- \rightarrow \gamma G_n$. It follows that the photon energy will be uniquely fixed by the well-known formula

$$E_\gamma = \frac{s - M_n^2}{2\sqrt{s}} \quad (5)$$

In practice, however, the graviton resonances need not be very narrow. The photon spectrum may be expected to show Breit-Wigner resonance peaks at positions given by the above equation for $n = 1, 2, \dots$. Observation of such resonances could constitute a clear signal of RS gravity.

As the RS graviton decay widths vary as c_0^2 (see Equation 6), in the limit of large c_0 , the decay widths are very large and the resonance peaks get smoothed out till they are no longer identifiable as resonances. One only sees a continuous photon spectrum (except for the Z -boson line, of course) with a clear excess over the SM. This is also precisely the kind of signal one would expect for the ADD model through the process $e^+e^- \rightarrow \gamma G_n$, where the ADD gravitons escape detection [6, 21]. In fact, as we shall see, the angular distribution of the photon also looks identical in both these models, and it seems difficult to disentangle the signals. We show, however, that by combining the signal for $e^+e^- \rightarrow \gamma \cancel{e}$ with that for the ‘benchmark’ process $e^+e^- \rightarrow \mu^+\mu^-$, we can still obtain a clear separation between the two models. This is an issue which has not been addressed before in the literature.

In the following section we briefly discuss the decays of RS gravitons and then go on to describe the long and cumbersome calculation of the $2 \rightarrow 3$ -body process $e^+e^- \rightarrow \gamma\nu\bar{\nu}$. Our numerical results, including discovery limits in the RS model parameter space, are presented in Section 3. In Section 4, we discuss how to disentangle signals for the RS model in the large c_0 limit from those for the ADD scenario. We summarize our results in Section 5 and relegate some important formulae to the Appendix.

2 Graviton Resonances and the Process $e^+e^- \rightarrow \gamma\nu\bar{\nu}$

As explained above, experimental searches for RS gravitons mainly focus on the fact that they can form narrow resonances in high-energy scattering processes. A simple calculation of the graviton width yields the form

$$\Gamma_n = c_0^2 x_n^3 m_0 \sum \Delta_{P\bar{P}}^{(n)} \quad (6)$$

where the sum \sum_P runs over all pairs of particles ($G_n \rightarrow P\bar{P}$) and the $\Delta_{P\bar{P}}^{(n)}$ are dimensionless functions of x_n and the ratios $r_P = m_P/m_0$.

In Figure 1, we show the region in the c_0 - m_0 plane for which the graviton resonances have widths less than 10 GeV. This is a reasonable estimate, taking likely experimental resolutions into account [16], of the sharpness required in order to identify resonances at the next generation of colliders, such as, for example, a 500 GeV linear collider. It is clear from the figure that for low values of c_0 the graviton widths remain quite small, leading to identifiable resonances. This is true for $n = 1$ for a large range of the parameter space considered, unless, indeed, $c_0 > 0.006$ and $m_0 \simeq 500$ GeV, in which case the width begins to cross 10 GeV. For $m_0 \leq 200$ GeV, we get sharp resonances for $n = 1$ for c_0 all the way up to 0.01. In any case, as the graph shows, very large widths are predicted only for regions with very large c_0 and rather small m_0 , which are already constrained by the Run-I dilepton data at the Tevatron [11, 15]. It is thus reasonable to expect the first massive graviton state to provide a sharp resonance peak, a fact which forms the basis of existing studies in the context of the LHC [22].

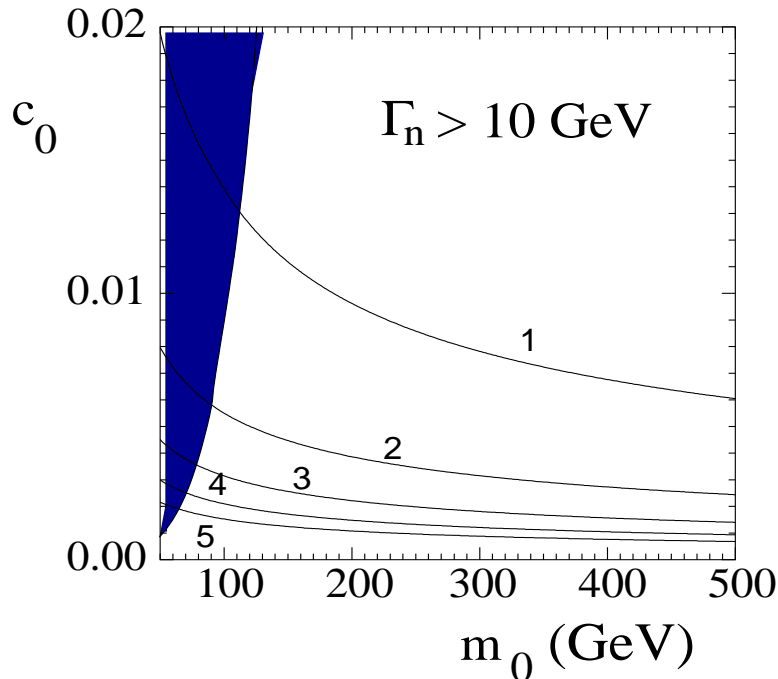


Figure 1. Illustrating the region (below the solid lines) in the parameter space of the RS model for which the graviton width remains small ($\Gamma_n < 10$ GeV), for the first five graviton resonances. The shaded region represents the constraints from dilepton production at the Tevatron.

The situation for the next two resonances is somewhat complicated. The figure makes it clear that we can expect resonance peaks, but not really sharp ones, for $n = 2, 3$ for low values of c_0 and m_0 around 100 GeV (i.e. $M_1 \approx 383$ GeV). However, as c_0 and m_0 increase, these widths grow steeply and soon the resonance shape is lost. For $n > 3$ this seems to be the case, even when c_0 and m_0 are small. We thus see that for suitable values of the parameters, it might be just possible to observe the first three graviton resonances in the RS model, but hardly more. In fact, most of the time, only two resonances will

be identifiable. Moreover, any analysis based on identifiable resonances, such as those in Ref. [22] will break down when all the resonances are wide, e.g. for $c_0 > 0.006$ and $m_0 > 200$ GeV.

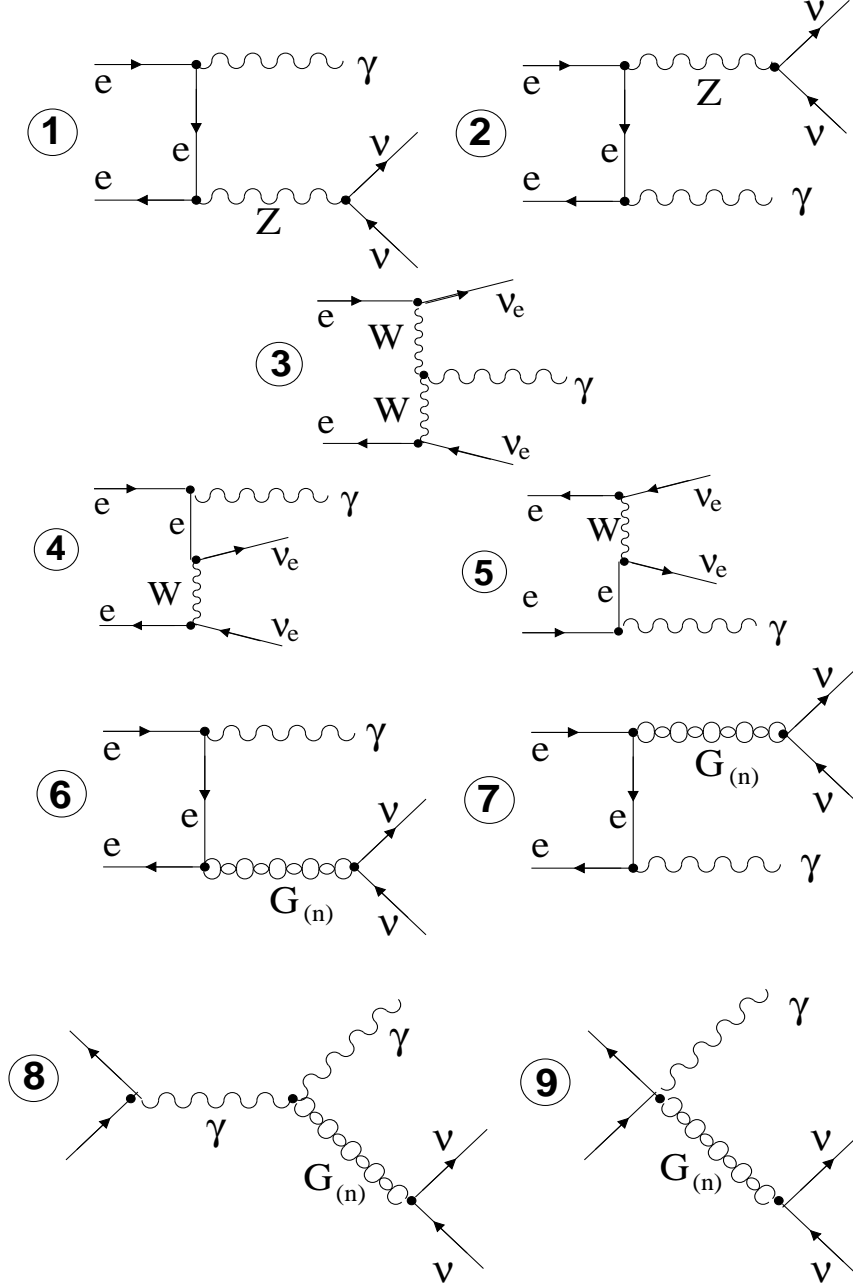


Figure 2. Feynman diagrams contributing to the process $e^+e^- \rightarrow \gamma\nu\bar{\nu}$ in the RS model. Diagrams numbered 1 to 5 are present in the SM model, while diagrams 6 to 9 involve graviton exchange. Diagrams numbered 3, 4 and 5 exist only for the electron neutrino.

We now concentrate on the $2 \rightarrow 3$ -body process

$$e^-(k_1, \lambda_1) + e^+(k_2, \lambda_2) \longrightarrow \gamma(p_1) + \bar{\nu}(p_2) + \nu(p_3)$$

which is observable as a final state with a single hard photon with unbalanced (missing) energy. Note that we display only the helicities of the initial states, as the (unobserved)

helicities of the final states will be summed over. Figure 2 shows the complete set of tree-level Feynman diagrams contributing to the process in the RS model. Of these diagrams numbered 1–5 exist in the SM, while those numbered 6–9 involve graviton exchanges and constitute the ‘new physics’ component. Diagrams 1–2, 6–9 are labeled with ν indicating a neutrino of *any* flavour, while diagrams 3–5 are specifically labeled with the electronic flavour ν_e . Feynman amplitudes corresponding to these nine diagrams are given in the Appendix.

We use these amplitudes to calculate the cross-section in terms of the usual $2 \rightarrow 3$ body invariants s, s_1, s_2, t_1 and t_2 . The expressions, including 36 possible interference terms, are long and messy. In the interests of brevity, we do not present them in this paper. The final cross-section was coded into a Monte Carlo event generator, which produced the numerical results. The graviton contributions require a summation over graviton Kaluza-Klein modes, parametrised by the function $\Lambda(Q^2)$, which is defined as

$$\Lambda(Q^2) = \sum_n \frac{\kappa^2 e^{2\pi\mathcal{K}Rc}}{Q^2 - M_n^2 + iM_n\Gamma_n} \quad (7)$$

where n runs over all the graviton modes. We now explain briefly how the function $\Lambda(Q^2)$ is evaluated.

As mentioned above, masses of the Kaluza-Klein gravitons in the RS model vary as $M_n = x_n m_0$ where x_n are the zeroes of the Bessel function $J_1(x)$. These may be approximated by [23]

$$x_1 \simeq 1.22\pi, \quad x_2 \simeq 2.23\pi, \quad x_n \approx x_2 + (n-2)\pi. \quad (8)$$

However, we have seen that the width Γ_n is a complicated function of the mass M_n . If we consider Breit-Wigner resonances up to $n = N$ and simple propagator summation thereafter, we get a simplified form

$$\begin{aligned} \Lambda(Q^2) &\approx 16\pi \frac{c_0^2}{m_0^2} \left[\sum_{n=1}^N \frac{1}{Q^2 - M_n^2 + iM_n\Gamma_n} + \sum_{n=N+1}^{\infty} \frac{1}{Q^2 - M_n^2} \right] \\ &= 16\pi \frac{c_0^2}{m_0^4} \left[\sum_{n=1}^N \frac{1}{x^2 - x_n^2 + ix_n\gamma_n} + \psi\left(\frac{x_2 + x}{\pi} + N - 1\right) - \psi\left(\frac{x_2 - x}{\pi} + N - 1\right) \right] \end{aligned} \quad (9)$$

where $x^2 = Q^2/m_0^2$, $\gamma_n = \Gamma_n/m_0$ and ψ is the Euler digamma function, which is obtained on performing the infinite sum of the remaining terms³. In our numerical analysis, we determine N by the simple criterion that for $n > N$, the Breit-Wigner contribution from a single resonance should not exceed 1% of the resonance value of $\Lambda(Q^2)$. Calculated in this way, we have checked that our results closely match those of, for example, Ref. [15].

³Strictly speaking, the sum is not infinite, but must be cut off at the five-dimensional Planck scale. However, this is so much larger than the experimental energy that the sum is, for all practical purposes, infinite.

3 Results and Discussion

Our numerical analysis of the problem has been performed for two values of center-of-mass energy, viz., $\sqrt{s} = 500$ GeV and $\sqrt{s} = 800$ GeV [16]. Noting that the final state consists of a single hard isolated photon, we impose the following kinematic cuts

- The photon should have energy $E_\gamma \geq 20$ GeV.
- The photon scattering angle θ_γ should satisfy $15^\circ \leq \theta_\gamma \leq 165^\circ$.

These ensure that the tagged photon does not arise from beamstrahlung or other similar sources [24]. Assuming 100% efficiency in photon detection (we shall see later that the actual efficiency factors cancel out), we then calculate the differential and total cross-section for both (a) unpolarised and (b) polarised beams.

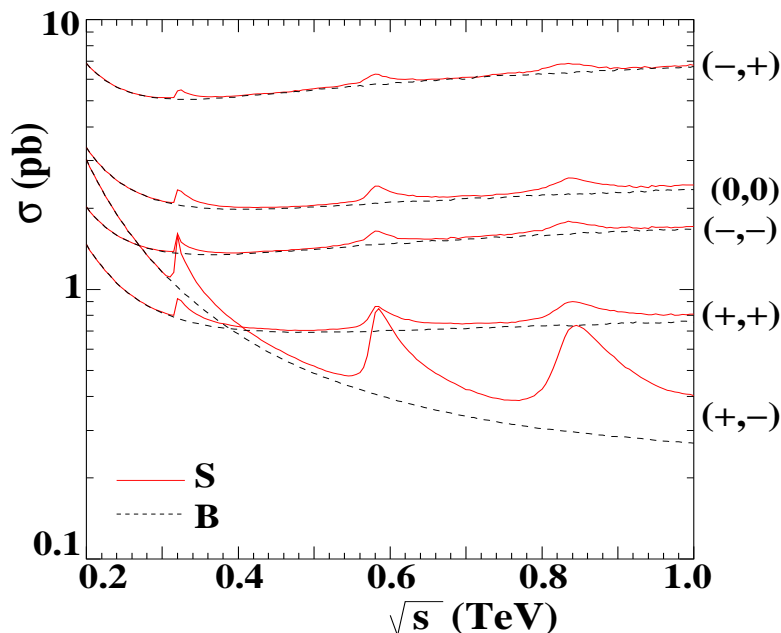


Figure 3. Illustrating the variation of signal (S) and background (B) with center-of-mass energy \sqrt{s} for different choices of $[\text{sgn}(P_e), \text{sgn}(P_p)]$. The choice (0,0) corresponds to unpolarised beams. Clearly the best choice is to take $\mathcal{P}_1 = 0.8$ and $\mathcal{P}_p = -0.6$. The signal was calculated taking $m_0 = 60$ GeV and $c_0 = 0.015$.

Beam polarisation can be an extremely efficient tool in reduction of the SM background (diagrams 1–5 in Figure 2). This is because the largest contributions to the signal arise from t -channel exchange of W -bosons in the process $e^+e^- \rightarrow \gamma\nu_e\bar{\nu}_e$ (diagrams 3–5). These diagrams are strongly suppressed if the electron (positron) beam is right (left) polarised, because of the $V - A$ nature of the W -boson coupling. This is beautifully illustrated in Figure 3, where we plot the total cross-section for $e^+e^- \rightarrow \gamma\nu\bar{\nu}$ (signal S and well as background B) against the center-of-mass energy \sqrt{s} . We show the unpolarised (0,0) case, as well as all four choices of $[\text{sgn}(P_e), \text{sgn}(P_p)]$ taking typical values [16] $|P_e| = 0.8$ and $|P_p| = 0.6$. It is apparent that the choice (+,-), corresponding to right (left)

polarised electron (positron), produces roughly an order-of-magnitude suppression of the background and thereby throws the new physics signal into prominence in a way that cannot be achieved otherwise. For the rest of this paper, then, we concentrate on this choice. Since the cross-section is still in the range of a few hundred femtobarns, and we expect [16] a luminosity of at least 10 fb^{-1} , this would mean a few thousand events, and more if the high-luminosity option of 1000 fb^{-1} is achieved. Thus, the use of beam polarisation turns out to be an unambiguous blessing.

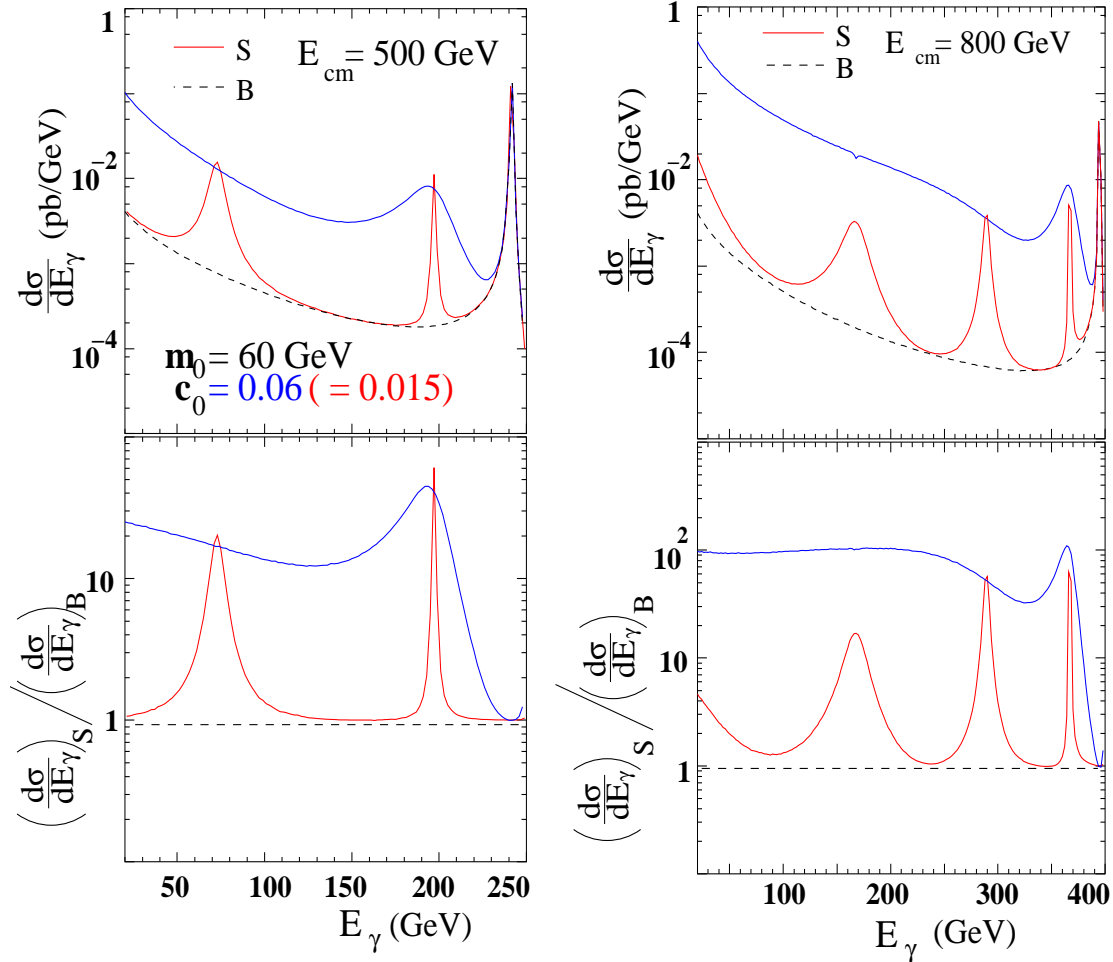


Figure 4. Energy spectrum of the tagged photon e for the parameter choices $m_0 = 60 \text{ GeV}$ and $c_0 = 0.015$ and 0.06 . S and B denote signal (SM plus gravitons) and background (SM only) respectively. Note that the right-most peak, which is due to the Z-boson, can be removed by taking the S/B ratio. We consider polarised beams with $\mathcal{P}_e = 0.8$ and $\mathcal{P}_p = -0.6$.

We can study the kinematic distributions of the only two measurables: the energy E_γ and the scattering angle θ_γ of the photon. In Figure 4, we display, for $\sqrt{s} = 500$ and 800 GeV respectively, the photon energy spectrum for both the signal and the SM background. The dashed (black) line represents the background (note the Z-boson peak toward the right end), while solid curves correspond to the signal for a low (red) and high (blue) value of the parameter c_0 . For this figure, we have chosen $m_0 = 60 \text{ GeV}$, which means that the first two (three) graviton resonances, at $230, 421$ and 609 GeV

respectively, are accessible to a machine running at a center-of-mass energy of 500 (800) GeV. Observe that the resonance peaks broaden as the order $n = 1, 2, \dots$ of the Kaluza-Klein excitation increases, and that, for larger values of c_0 , the resonance line-shape merges into a continuous spectrum.

In the upper halves of the two graphs in Figure 4, we display the differential cross-section for the process $e^+e^- \rightarrow \gamma + \cancel{E}$. The bottom halves show the same distribution, except that now we exhibit the signal-to-background (S/B) ratio. Not only does this remove the uninteresting Z -peak, but it also takes care of any radiative corrections, efficiency factors, etc, which can be written in a factorisable form.

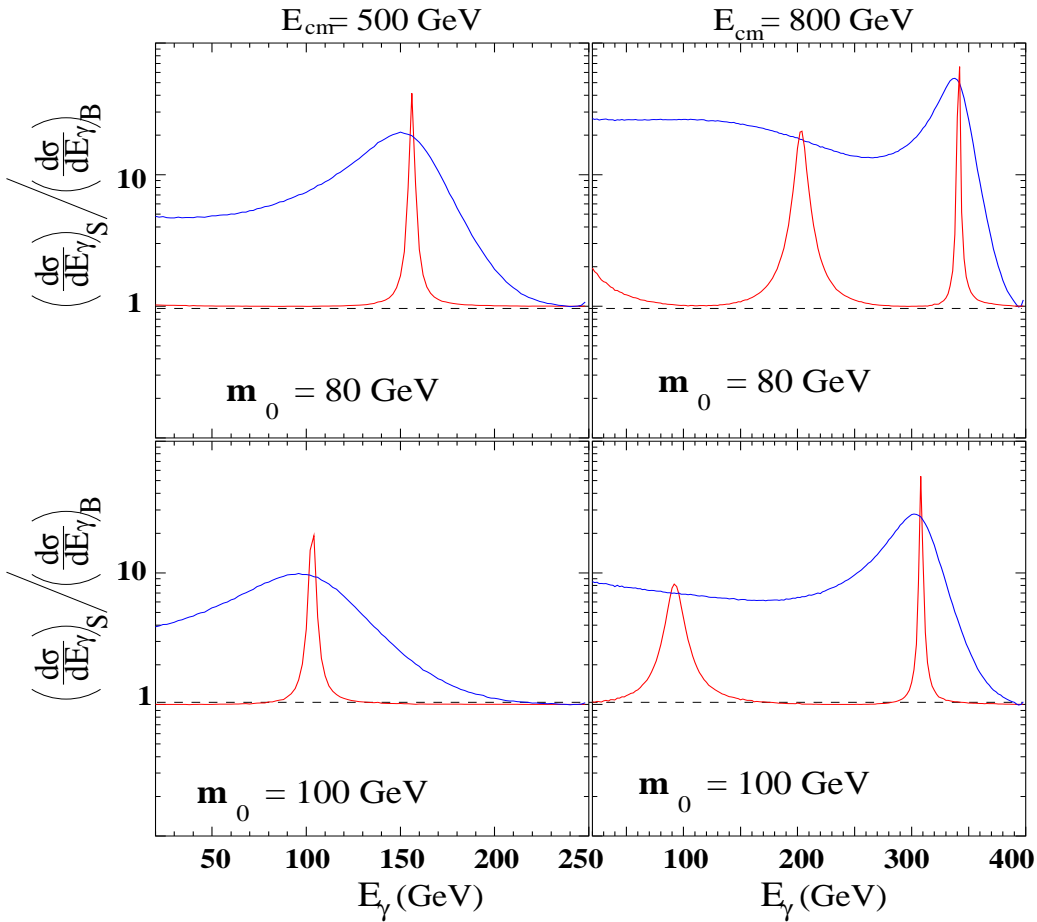


Figure 5. *Illustrating the shift and disappearance of resonance peaks with increasing m_0 . Notations and conventions are exactly as in Figure 4.*

In Figure 5, we exhibit similar signal-to-background ratios for larger values of m_0 , when the resonances become heavier. The first three graviton resonances lie at 306 (383), 561 (702) and 813 (1016) GeV respectively for $m_0 = 80$ (100) GeV. We observe that for $\sqrt{s} = 500$ GeV, only one resonance is kinematically accessible, while for $\sqrt{s} = 800$ GeV, two resonances would still be seen. It is simple to show that for $m_0 = 130$ (209) GeV, even the lightest resonance would become kinematically inaccessible.

Thus, we can expect one of the following possibilities.

- Case I: *Two (or more) clear resonances are seen in the photon spectrum*, or rather, in the signal-to-background ratio. This would correspond to a relatively low value of m_0 and a small value of c_0 , and would constitute a strong hint of RS gravity. For confirmation, we need to check two more details. First, the peak at smaller E_γ should be lower and broader than that at larger E_γ , as illustrated in Figures 4 and 5. This is because $\Gamma_n \propto x_n^3$. Secondly, the positions of the two resonances will bear a definite relation if they are due to RS gravitons. Using Equation (5) this works out to the requirement that, for resonance values $E_\gamma^{(1)} > E_\gamma^{(2)}$,

$$\sqrt{\frac{\sqrt{s} - 2E_\gamma^{(1)}}{\sqrt{s} - 2E_\gamma^{(2)}}} = \frac{M_1}{M_2} = \frac{x_1}{x_2} \simeq 0.546 . \quad (10)$$

It would be a very remarkable coincidence, indeed, if some other form of new physics⁴ — such as, for example, two extra Z' bosons — could reproduce this ratio. Thus, if we do see two clear resonances, *satisfying the above relation*, it be quite in order to claim this as a ‘smoking gun’ signal for the RS model (or a close variation).

- Case II: *One sharp resonance is seen, but no more*. If this is a graviton resonance, it will correspond to a somewhat larger value of m_0 when only the first (lightest) graviton resonance is kinematically accessible. A single resonance could also indicate the presence of some other kind of new physics, such as, for example, an extra Z' boson, or perhaps a leptophilic scalar. Of course, one can still measure the position, width and height of the resonance, which would be fitted with just two parameters m_0 and c_0 . A consistent fit would constitute circumstantial evidence for RS gravitons, but would hardly be conclusive. However, in the case of RS gravitons, we should also expect extra contributions to 2-body final states such as $\mu^+\mu^-$, and the angular distribution of these might be useful to distinguish between different types of new physics.
- Case III: *No resonances are seen, but large excesses in the S/B ratio are observed*. This could be due to RS gravitons with a large coupling c_0 , which means smeared-out resonances. However, it could also be due to various other sources, such as ADD gravitons (which form a near-continuous spectrum), or, perhaps the production of supersymmetric particles. A process like $e^+e^- \rightarrow \gamma\tilde{\chi}_1^0\tilde{\chi}_1^0$, where $\tilde{\chi}_1^0$ is the (invisible) lightest neutralino, would contribute [18, 19] an excess very similar to the observed one. In this case, it may be a real challenge to determine the nature of the new physics causing this signal. In the next section we take up the issue of separating ADD versus RS graviton signals with comparable kinematic signatures. However, the comparison with supersymmetry and other types of new physics is a tricky issue, very much dependent on the choice of model parameters, and it is premature, at this point of time, to take up a detailed investigation.

⁴Barring variations of the RS model which put SM fields in the bulk [25]. The authors are grateful to K. Sridhar for pointing out this feature.

- Case IV: *No excess is seen: the observed spectrum is completely consistent with the SM prediction.* This possibility would be rather disappointing, but it can hardly be ignored for that reason. In such a case, we would argue that the RS gravitons are too heavy to be kinematically accessible to the linear collider. We would then get as bounds what we now present in Figure 6 as 95% confidence level discovery limits.

In order to obtain the discovery limits shown in Figure 6, we have to take into account any excess in the differential cross-section ratio shown in Figures 4 and 5, irrespective of whether a resonance is discernible or not. To do this, we make a simple-minded χ^2 analysis of the bin-wise energy distribution of the photon, and indicate the region of the parameter space where a departure from the SM prediction would be observable at 95% confidence level. Figure 6 clearly illustrates how far a high energy linear collider can probe the RS model. Compared with the bound from Tevatron Run-I dilepton data [11, 15] we see that a linear collider can probe much larger values of m_0 , i.e. graviton resonances which are many times heavier.

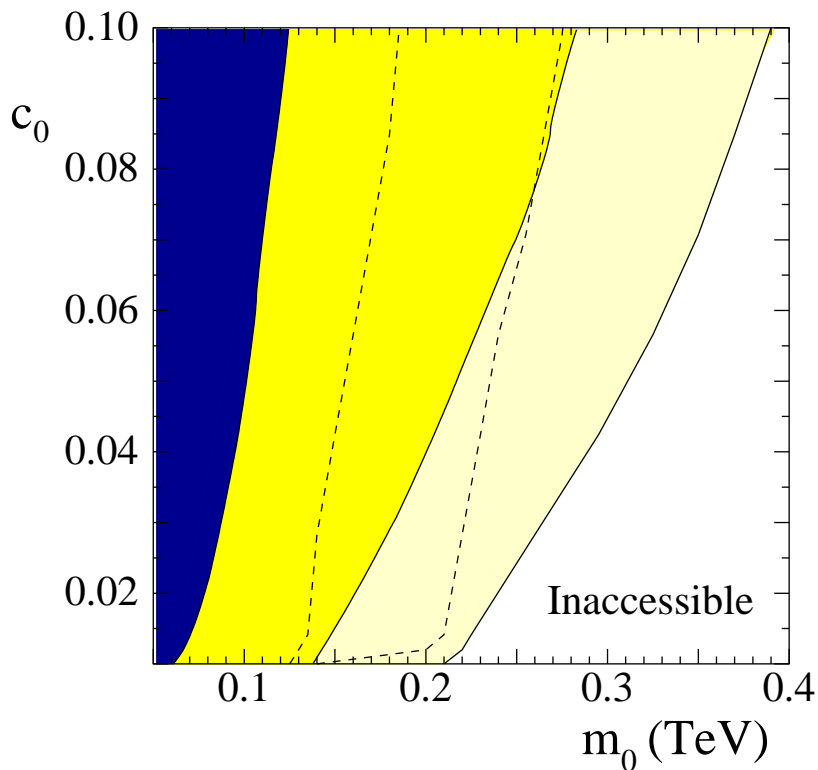


Figure 6. Discovery limits at 95% C.L. for the RS model in the c_0 - m_0 plane using single-photon signals. The region shaded dark blue is the Tevatron bound from dileptons. The regions shaded light (dark) yellow correspond to $\sqrt{s} = (500) 800$ GeV and high luminosity ($\mathcal{L} = 10^3$ fb $^{-1}$). Broken lines correspond to low luminosity ($\mathcal{L} = 10$ fb $^{-1}$).

4 Distinguishing between RS and ADD Models

We now come to the crucial issue: when the coupling c_0 is large, and no clear resonance structure is visible, is it possible to distinguish between the $\gamma + \cancel{E}$ signal arising from

RS graviton from those arising from ADD gravitons [6, 21]. we have already explained that not much can then be gained from a study of the photon energy spectrum. The only other observable is the photon angular distribution $d\sigma/d\theta_\gamma$. In the ADD model, the signal arises from $2 \rightarrow 2$ -body processes corresponding to diagrams similar to nos. 6–9 in Figure 2, but without the neutrino lines. Hence, there is no interference with the SM diagrams and this could be expected to lead to some difference in the angular distribution of the photon.

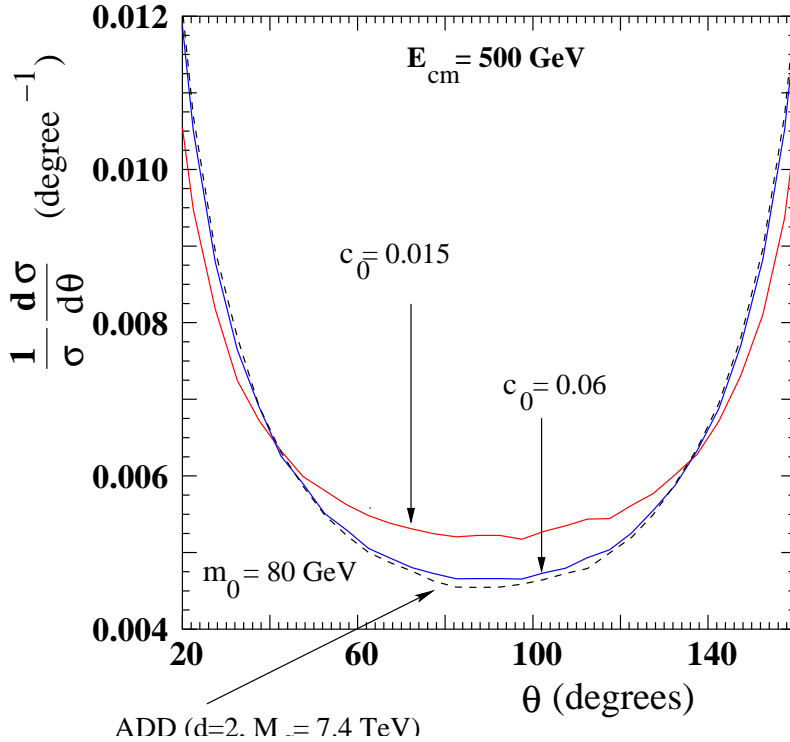


Figure 7. Normalized angular distribution of single photons in the RS (solid lines) and ADD (broken line) models for $\sqrt{s} = 500$ GeV. Parameters choices are marked on the figure itself.

In Figure 7, we display the (normalized) photon angular distribution at a 500 GeV collider for the following cases:

1. RS gravitons, with $m_0 = 80$ GeV and $c_0 = 0.015$, indicated with a solid red line;
2. RS gravitons, with $m_0 = 80$ GeV and $c_0 = 0.06$, indicated with a solid blue line;
3. ADD gravitons with $d = 2$ and $M_S = 7.4$ TeV, indicated with a broken black line.

It is apparent from the figure that the first case shows a somewhat different (though not dramatically so) distribution from the others. However, since c_0 is small, this is also the case when resonances will be discernible in the energy spectrum. The choice of parameters for the second and third lines is governed by the requirement that the energy spectrum should look indistinguishable. Unfortunately, as Figure 7 makes clear, in this case, the angular distributions also look almost identical and it is unlikely, given that there will be experimental errors, that we can make a distinction between these two cases on the basis of the angular distribution.

It is clear, therefore, that a study of the process $e^-e^+ \rightarrow \gamma\nu\bar{\nu}$ alone cannot clearly distinguish between the ADD and RS models, should a continuous excess in the photon spectrum be observed. However, if we consider this process *in conjunction* with a benchmark process, like $e^+e^- \rightarrow \mu^+\mu^-$, for example, we do find a marked difference. This is because the $\gamma + \cancel{E}$ signal arises in the ADD model from a $2 \rightarrow 2$ -body process, whereas in the RS model it arises from a $2 \rightarrow 3$ -body process, which is phase-space suppressed. Consequently, when the cross-sections for the two match, the ADD parameter M_S must be rather large, as is evidenced by the choice 7.4 TeV in Figure 7. When we consider the corresponding contributions to a $2 \rightarrow 2$ body process, like $e^+e^- \rightarrow \mu^+\mu^-$, the same choice of parameters would yield a much larger cross-section for the RS model. Using this idea as a cue, in Figure 8 we plot our predictions, at a 500 GeV machine, for $\sigma(e^+e^- \rightarrow \gamma\cancel{E})$ versus $\sigma(e^+e^- \rightarrow \mu^+\mu^-)$ for both the models in question. For the RS model, we choose three values $m_0 = 70, 80$ and 90 GeV, and vary the value of c_0 between 0.01 and 0.1, which is the expected range. For the ADD model we have varied M_S from \sqrt{s} to much larger values, for $d = 2, 4$ and 6 . The broken red line shows the region (below the line) where the RS graviton width crosses 10 GeV and produces broad resonances.

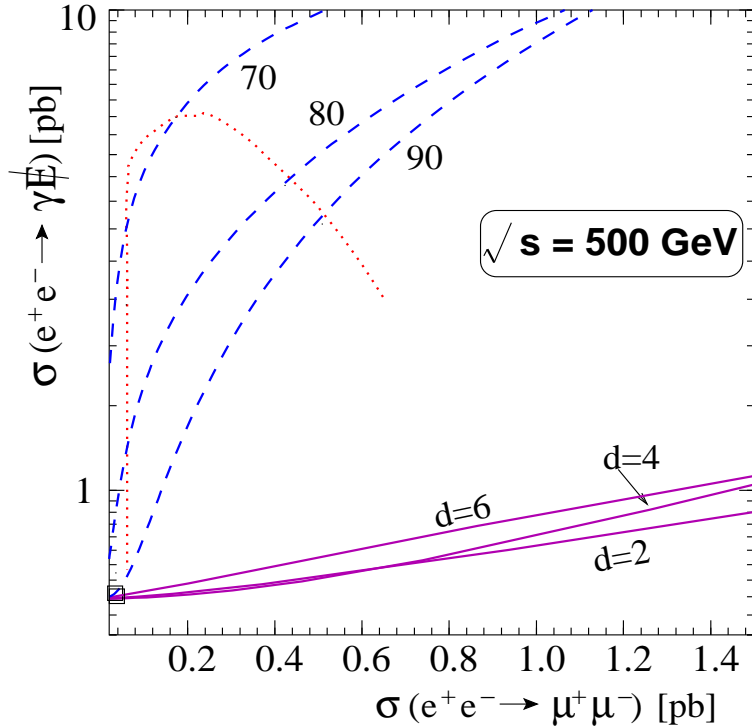


Figure 8. Correlation plot showing the cross-section for the single photon signal vis-à-vis the cross-section for muon pair-production. Solid (magenta) lines correspond to the ADD model for three (marked) values of d , while broken (blue) lines correspond to the RS model for three values of m_0 (marked, in GeV). The dotted (red) line demarcates the non-resonant region.

A glance at Figure 8 makes it obvious that a correlation plot of this nature shows a clear difference between ADD and RS models. If the actual observation point is found to lie toward the upper-left corner of the graph, one could clearly say that the signal is of RS gravity. If the observation point were to lie toward the bottom-right corner of the graph,

it would be equally certain that the signal must come from ADD gravity. If, however, the point comes out close to the bottom-left corner, where the two sets of graphs merge into the SM prediction, it will be difficult to distinguish any kind of new physics effect at all.

A correlation plot such as that shown in Figure 8 could, in fact, prove more useful than merely in distinguishing between ADD and RS models. If we consider a supersymmetric model, such as the minimal supersymmetric SM, for example, we will not predict extra contributions to $e^+e^- \rightarrow \mu^+\mu^-$. In that case, the observed point will lie on the vertical axis of Figure 8, and may be distinguished from the graviton contributions if the errors are small enough. Contributions from one (or more) extra Z' bosons would look similar to the RS graviton contributions, but would be distinguishable by the existence of clear resonances in the photon spectrum, since Z' widths are usually small. We have already discussed how to distinguish between graviton and Z' resonances.

5 Summary and Conclusions

To summarize then, it is quite evident that, like supersymmetric models, solutions of the hierarchy problem which require the existence of extra hidden dimensions are here to stay. It is, therefore, of great interest to investigate their phenomenological conclusions. In this paper, we have investigated the process $e^+e^- \rightarrow \gamma\nu\bar{\nu}$ in the (minimal) Randall-Sundrum model of warped quantum gravity. This process has a clean signature, since the final observed state consists of a single hard photon with unbalanced momentum. We show that the energy spectrum of this photon could show clear resonances corresponding to massive gravitons, and discuss how these can be distinguished from other forms of new physics yielding resonances. We then consider the large-coupling limit of the RS model, where the resonances are smeared out and the photon spectrum is practically indistinguishable from that predicted by the ADD model with large extra dimensions. We demonstrate that a correlation plot between the cross-sections for $e^+e^- \rightarrow \gamma \cancel{E}$ and a benchmark process like $e^+e^- \rightarrow \mu^+\mu^-$ can be used to make a clear demarcation, not only between signals for RS and ADD gravitons, but also between other kinds of new physics. This addresses an issue which has not been discussed in any detail before and suggests an elegant and easy-to-perform test, which uses cross-sections which are almost certain to be measured when a high-energy linear collider actually goes into operation.

Acknowledgments

This work constitutes part of the activities of the Indian Linear Collider Working Group (ILCWG) under Project No. SP/S2/K-01/2000-II, of the Department of Science & Technology, Government of India. The authors thank Sunanda Banerjee, Debajyoti Choudhury, Saurabh D. Rindani and K. Sridhar for discussions.

Appendix: Decay width and Cross-section formulae

In this Appendix, we collect some useful formulae which are necessary to evaluate the graviton cross-sections discussed in the text.

§ *Graviton decay*; The dimensionless functions $\Delta_{P\bar{P}}^{(n)}$ required to calculate the graviton partial widths are listed below:

$$\begin{aligned}
\Delta_{\gamma\gamma}^{(n)} &= \frac{1}{5} \\
\Delta_{gg}^{(n)} &= \frac{8}{5} \\
\Delta_{WW}^{(n)} &= \frac{2}{5} \sqrt{1-4x_W^2} \left(\frac{13}{12} + \frac{14}{39}r_W + \frac{4}{13}r_W^2 \right) \theta(x_n - 2r_W) \\
\Delta_{ZZ}^{(n)} &= \frac{1}{5} \sqrt{1-4x_Z^2} \left(\frac{13}{12} + \frac{14}{39}r_Z + \frac{4}{13}r_Z^2 \right) \theta(x_n - 2r_Z) \\
\Delta_{HH}^{(n)} &= \frac{1}{30} (1-4x_H^2)^{5/2} \theta(x_n - 2r_H) \\
\Delta_{\nu\bar{\nu}}^{(n)} &= \frac{1}{10} \\
\Delta_{\ell\bar{\ell}}^{(n)} &= \frac{1}{10} (1-4x_\ell^2)^{3/2} \left(1 + \frac{8}{3}r_\ell \right) \theta(x_n - 2r_\ell) \\
\Delta_{q\bar{q}}^{(n)} &= \frac{3}{10} (1-4x_q^2)^{3/2} \left(1 + \frac{8}{3}r_q \right) \theta(x_n - 2r_q)
\end{aligned} \tag{11}$$

where $r_P = m_P/m_0$ for every SM particle P . These formulae are consistent with those presented in Ref. [7]. When using the above formulae we must remember to sum over three neutrino flavours ν , three charged leptons ℓ and six quarks q . The colour factor for quarks is already included.

§ *Single photon production*: The amplitudes corresponding to the 9 different Feynman diagrams in Figure 2 are given below. Helicities of the final states are not exhibited explicitly, as these will be summed over. We have used the Feynman rules and notations given in Ref. [7].

$$\begin{aligned}
M_1 &= \frac{ieg^2}{16 \cos^2 \theta_W} \frac{1}{(k_1 - p_1)^2} \frac{1}{(p_2 + p_3)^2 - M_Z^2 + iM_Z\Gamma_Z} \varepsilon_\mu^*(p_1) \\
&\quad \times \bar{v}(k_2, \lambda_2) \gamma^\alpha (c_V - \gamma_5) (\not{k}_1 - \not{p}_1) \gamma^\mu u(k_1, \lambda_1) \cdot \bar{u}(p_2) \gamma_\alpha (1 - \gamma_5) v(p_3)
\end{aligned} \tag{12}$$

$$\begin{aligned}
M_2 &= \frac{-ieg^2}{16 \cos^2 \theta_W} \frac{1}{(k_2 - p_1)^2} \frac{1}{(p_2 + p_3)^2 - M_Z^2 + iM_Z\Gamma_Z} \varepsilon_\mu^*(p_1) \\
&\quad \times \bar{v}(k_2, \lambda_2) \gamma^\mu (\not{k}_2 - \not{p}_1) \gamma^\alpha (c_V - \gamma_5) u(k_1, \lambda_1) \cdot \bar{u}(p_2) \gamma_\alpha (1 - \gamma_5) v(p_3)
\end{aligned} \tag{13}$$

$$\begin{aligned}
M_3 &= \frac{-ieg^2}{8} \frac{1}{(k_1 - p_2)^2 - M_W^2} \frac{1}{(k_2 - p_3)^2 - M_W^2} \\
&\quad \{ (k_1 - k_2 - p_2 + p_3)^\mu \eta^{\nu\lambda} + (k_2 + p_1 - p_3)^\nu \eta^{\lambda\mu} - (k_1 + p_1 - p_2)^\lambda \eta^{\mu\nu} \} \varepsilon_\mu^*(p_1) \\
&\quad \times \bar{v}(k_2, \lambda_2) \gamma_\lambda (1 - \gamma_5) v(p_3) \cdot \bar{u}(p_2) \gamma_\nu (1 - \gamma_5) u(k_1, \lambda_1)
\end{aligned} \tag{14}$$

$$\begin{aligned}
M_4 &= \frac{-ieg^2}{8} \frac{1}{(k_1 - p_1)^2} \frac{1}{(k_2 - p_3)^2 - M_W^2} \varepsilon_\mu^*(p_1) \\
&\quad \times \bar{v}(k_2, \lambda_2) \gamma^\alpha (1 - \gamma_5) v(p_3) \cdot \bar{u}(p_2) \gamma_\alpha (1 - \gamma_5) (\not{k}_1 - \not{p}_1) \gamma^\mu u(k_1, \lambda_1)
\end{aligned} \tag{15}$$

$$\begin{aligned}
M_5 &= \frac{ieg^2}{8} \frac{1}{(k_2 - p_1)^2} \frac{1}{(k_1 - p_2)^2 - M_W^2} \varepsilon_\mu^*(p_1) \\
&\quad \times \bar{v}(k_2, \lambda_2) \gamma^\mu (\not{k}_2 - \not{p}_1) \gamma^\alpha (1 - \gamma_5) v(p_3) \cdot \bar{u}(p_2) \gamma_\alpha (1 - \gamma_5) u(k_1, \lambda_1)
\end{aligned} \tag{16}$$

$$\begin{aligned}
M_6 &= \frac{ie}{128} \Lambda(Q^2) \frac{1}{(k_1 - p_1)^2} \varepsilon_\mu^*(p_1) P_{\alpha\beta\rho\sigma}(Q) \\
&\quad \times \bar{v}(k_2, \lambda_2) \{ \gamma^\alpha (k_1 - k_2 - p_1)^\beta + \gamma^\beta (k_1 - k_2 - p_1)^\alpha - 2\eta^{\alpha\beta} (\not{k}_1 - \not{p}_1) \} (\not{k}_1 - \not{p}_1) \gamma^\mu u(k_1, \lambda_1) \\
&\quad \times \bar{u}(p_2) \{ \gamma^\rho (p_2 - p_3)^\sigma + \gamma^\sigma (p_2 - p_3)^\rho \} v(p_3) \tag{17}
\end{aligned}$$

$$\begin{aligned}
M_7 &= \frac{-ie}{128} \Lambda(Q^2) \frac{1}{(k_2 - p_1)^2} \varepsilon_\mu^*(p_1) P_{\alpha\beta\rho\sigma}(Q) \\
&\quad \times \bar{v}(k_2, \lambda_2) \gamma^\mu (\not{k}_2 - \not{p}_1) \{ \gamma^\alpha (k_1 - k_2 + p_1)^\beta + \gamma^\beta (k_1 - k_2 + p_1)^\alpha + 2\eta^{\alpha\beta} (\not{k}_2 - \not{p}_1) \} u(k_1, \lambda_1) \\
&\quad \times \bar{u}(p_2) \{ \gamma^\rho (p_2 - p_3)^\sigma + \gamma^\sigma (p_2 - p_3)^\rho \} v(p_3) \tag{18}
\end{aligned}$$

$$\begin{aligned}
M_8 &= \frac{ie}{32} \Lambda(Q^2) \frac{1}{(k_1 + k_2)^2} \varepsilon_\mu^*(p_1) P_{\alpha\beta\rho\sigma}(Q) \{ (k_1 + k_2) \cdot p_1 C^{\alpha\beta\mu\nu} + D^{\alpha\beta\mu\nu} \} \\
&\quad \times \bar{v}(k_2, \lambda_2) \gamma_\nu u(k_1, \lambda_1) \cdot \bar{u}(p_2) \{ \gamma^\rho (p_2 - p_3)^\sigma + \gamma^\sigma (p_2 - p_3)^\rho \} v(p_3) \tag{19}
\end{aligned}$$

$$\begin{aligned}
M_9 &= \frac{-ie}{64} \Lambda(Q^2) \varepsilon_\mu^*(p_1) P_{\alpha\beta\rho\sigma}(Q) \{ C^{\alpha\beta\mu\lambda} - \eta^{\alpha\beta} \eta^{\mu\lambda} \} \\
&\quad \times \bar{v}(k_2, \lambda_2) \gamma_\lambda u(k_1, \lambda_1) \cdot \bar{u}(p_2) \{ \gamma^\rho (p_2 - p_3)^\sigma + \gamma^\sigma (p_2 - p_3)^\rho \} v(p_3) \tag{20}
\end{aligned}$$

where $c_V = 1 - 4 \sin^2 \theta_W \simeq 0.074$. The sum over graviton polarisations reduces, when the graviton couples to a conserved current with massless fermions, to the simple form

$$P_{\mu\nu\rho\sigma}(Q) = \eta_{\mu\rho} \eta_{\nu\sigma} + \eta_{\nu\rho} \eta_{\mu\sigma} \tag{21}$$

where $Q = p_2 + p_3$ is the momentum carried by the graviton propagator. The tensor couplings $C^{\alpha\beta\mu\nu}$ and $D^{\alpha\beta\mu\nu}$ are given by

$$\begin{aligned}
C^{\alpha\beta\mu\nu} &= \eta^{\alpha\mu} \eta^{\beta\nu} + \eta^{\alpha\nu} \eta^{\beta\mu} - \eta^{\alpha\beta} \eta^{\mu\nu} \tag{22} \\
D^{\alpha\beta\mu\nu} &= \eta^{\alpha\beta} p_1^\nu (k_1 + k_2)^\mu - \left\{ \eta^{\alpha\nu} p_1^\beta (k_1 + k_2)^\mu + \eta^{\alpha\mu} p_1^\nu (k_1 + k_2)^\beta - \eta^{\mu\nu} p_1^\alpha (k_1 + k_2)^\beta \right\} \\
&\quad - \{ \alpha \leftrightarrow \beta \}
\end{aligned}$$

following Ref. [7]. The function $\Lambda(Q^2)$ is discussed in the text (Section 2).

References

- [1] K. Akama, *Lect. Notes Phys.* **176**, 267 (1982); V. Rubakov and M. Shaposhnikov, *Phys. Lett.* **B125**, 136 (1984) ; A. Barnaveli and O. Kancheli, *Sov. J. Nucl. Phys.* **51**, 573 (1990); I. Antoniadis, *Phys. Lett.* **B246**, 377 (1990) ; I. Antoniadis, C. Muñoz and M. Quiros, *Nucl. Phys.* **B397**, 515 (1993) ; I. Antoniadis, K. Benakli and M. Quiros, *Phys. Lett.* **B331**, 313 (1994) .
- [2] G. Nordström, *Phys. Zeitschr.*, **15**, 504 (1914); T. Kaluza, *Sitz. Preuss. Akad. Wiss. Berlin* **K1**, 966 (1921); O. Klein, *Z.Phys.* **37**, 895 (1926).
- [3] See, for example, J. Polchinski, *Tasi Lectures on D-Branes*, hep-th/9611050 (1996).
- [4] N. Arkani-Hamed, S. Dimopoulos and G. Dvali, *Phys. Lett.* **B429**, 263 (1998) ; I. Antoniadis, N. Arkani-Hamed, S. Dimopoulos and G. Dvali, *Phys. Lett.* **B463**, 257 (1998) ; N. Arkani-Hamed, S. Dimopoulos and G. Dvali, *Phys. Rev.* **D59**, 086004 (1999) .
- [5] J.C. Long *et al*, *Nature*, **421**, 922 (2003).
- [6] G.F. Giudice, R. Rattazzi and J.D. Wells, *Nucl. Phys.* **B544**, 3 (1998) .
- [7] T. Han, J.D. Lykken and R.-J. Zhang, *Phys. Rev.* **D59**, 105006 (1999) .
- [8] For a very readable review, see, for example, Y.A. Kubyshin, hep-ph/0111027 (2001).
- [9] L. Randall and R. Sundrum, *Phys. Rev. Lett.* **83**, 3370 (1999) .
- [10] W.D. Goldberger and M.B. Wise, *Phys. Rev.* **D60**, 107505 (1999) .
- [11] H. Davoudiasl, J.L. Hewett and T.G. Rizzo, *Phys. Rev. Lett.* **84**, 2080 (2000) .
- [12] T.G. Rizzo, SLAC preprint SLAC-PUB-9489 (2002), hep-ph/0209065; SLAC preprint SLAC-PUB-8959 (2001), hep-ph/0108235.
- [13] P. Das, S. Raychaudhuri, S. Sarkar, *JHEP*, **0007**, 050 (2000).
- [14] D.K. Ghosh and S. Raychaudhuri, *Phys. Lett.* **B495**, 114 (2000) .
- [15] H. Davoudiasl, J.L. Hewett and T.G. Rizzo, *Phys. Rev.* **D63**, 075004 (2001) .
- [16] ECFA/DESY LC Physics Working Group Report, J.A. Aguilar-Savedra *et al*, hep-ph/0106315 (2001); Snowmass Report, S. Kuhlman *et al*, hep-ex/9605011 (1996).
- [17] T.G. Rizzo, *JHEP*, **0306**, 021 (2003).
- [18] K. Grassie and P.N. Pandita, *Phys. Rev.* **D30**, 22 (1984) .

- [19] A. Datta, A.K. Datta and S. Raychaudhuri, *Phys. Lett.* **B349**, 113 (1995) ;
Eur. Phys. J. **C1**, 375 (1998)
- [20] A. Ghosal, A. Kundu and B. Mukhopadhyaya, *Phys. Rev.* **D56**, 504 (1997) ;
Phys. Rev. **D57**, 1972 (1998) .
- [21] E.A. Mirabelli, M. Perelstein and M.E. Peskin, *Phys. Rev. Lett.* **82**, 2236 (1999) .
- [22] B.C. Allanach *et al*, *JHEP*, **0212**, 039 (2002); P. Traczyk and G. Wrochna, Warsaw preprint, hep-ex/0207061.
- [23] See, for example, M. Abramowitz and I.E. Stegun, *Handbook of Mathematical Functions*, US National Bureau of Standards, Washington (1972).
- [24] C.H. Chen, M. Drees and J.F. Gunion, *Phys. Rev. Lett.* **76**, 2002 (1995) .
- [25] T.G. Rizzo, in *Les Houches 2001, Physics at TeV colliders*, p.245 (2001).